Письма в ЭЧАЯ. А. 2011. Т. 8, № 9. С. 169–173

DESCRIPTION OF pp COLLISIONS AT LHC ENERGIES

L. Bravina [a], *J. Bleibel* [b,c], *E. Zabrodin* [a,d]

[a] Department of Physics, University of Oslo, Oslo

[b] Institut für Physik, Johannes Gutenberg Universität Mainz, Mainz, Germany

[c] Max-Planck-Institut für Metallforschung, Stuttgart, Germany

[d] Institute of Nuclear Physics, Moscow State University, Moscow

The Monte Carlo version of quark–gluon string model is employed to study the multiplicity, rapidity and p_T spectra of particles in pp collisions at energies from $\sqrt{s} = 200$ GeV to 14 TeV. A good quantitative agreement with the experimental data is found in a broad energy range. It means that the general features of ultrarelativistic pp interactions can be well understood in terms of soft and hard Pomeron exchanges. Predictions are made for the top LHC energy $\sqrt{s} = 14$ TeV.

PACS: 13.75.Cs; 13.85.-t

INTRODUCTION

The raise of interest to general characteristics of ultrarelativistic proton–proton (pp) interactions is caused by several reasons. Namely, the partonic matter, produced in pp collisions at energies of several TeV accessible for the LHC at CERN, is so hot and dense that can reveal collective effects attributed to the formation of the quark–gluon plasma (QGP) in heavy-ion collisions. Note that up to now elementary pp interactions are used as reference for comparison with $A + A$ collisions. Also, the multiparticle production in hadronic and nuclear interactions cannot be described solely in terms of perturbative QCD. Here the dominant contribution even at very high energies comes from the «soft» processes with small momentum transfer. At large distances ($r \geqslant 1/\Lambda_{\rm QCD}$), or, equivalently, at small Q^2, the running coupling constant $\alpha_S(Q^2)$ is not small. Therefore, nonperturbative methods should be employed.

One of a few methods, which allow us to treat the nonperturbative effects in QCD, is based on the so-called $1/N$-expansion, where N is the number of colors or flavors. This approach is often dubbed topological expansion, because the various graphs arising in the $1/N$-expansion have certain topologies, such as plane, cylinder, etc. Whereas the weights of different graphs corresponding to their contribution to the total cross section of the reaction cannot be calculated within the $1/N$-expansion, all emerging diagrams can be treated as Feynman diagrams in perturbative Gribov's Reggeon field theory (GRT) [1], which is, therefore, linked to quantum chromodynamics. Thus, the GRT is a powerful tool to study processes of multiple particle production in relativistic hadronic and nuclear collisions.

The quark–gluon string model (QGSM) [2] is close to the dual parton model (DPM) [3]. Both models are based on the GRT and, therefore, obey both analyticity and unitarity requirements. In the present paper we employ the Monte Carlo version of the QGSM in order to study the general features of particle production in elementary pp collisions at ultrarelativistic energies. The model aspects are discussed in Sec. 1.

1. MC QUARK–GLUON STRING MODEL

The MC QGSM [4] is based on Gribov's Reggeon field theory accomplished by a string phenomenology of particle production in inelastic hadron–hadron (hh) collisions. To describe hadron–nucleus and nucleus–nucleus collisions, the cascade procedure of multiple secondary interactions of hadrons was implemented. The model incorporates the string fragmentation, formation of resonances, and rescattering of hadrons, but simplifies the nuclear effects neglecting, e.g., the mean fields or evaporation from spectators. As independent degrees of freedom QGSM includes octet and decuplet baryons, and nonets of vector and pseudoscalar mesons, and their antiparticles. Pauli blocking of occupied final states is taken into account. Strings in the QGSM can be produced as a result of the color exchange mechanism or, like in diffractive scattering, due to momentum transfer. The Pomeron, which is a pole with an intercept $\alpha_P(0) > 1$ in the GRT, corresponds to the cylinder-type diagrams. The s-channel discontinuities of the diagrams, representing the exchange by n-Pomerons, are related to process of $2k\,(k \leqslant n)$ string production. If the contributions of all n-Pomeron exchanges to the forward elastic scattering amplitude are known, the AGK cutting rules [5] enable one to determine the cross sections for $2k$-strings.

The statistical weights, hadron structure functions and leading quark fragmentation functions have been obtained from the Regge approach to choose subprocesses of string production, to compute mass and momentum of strings and to simulate string decays, respectively. These include subprocesses with quark annihilation and quark exchange, connected to Reggeon exchanges in two-particle amplitudes in Regge theory, and with color exchange, connected with the one and more Pomeron exchanges in elastic amplitudes in Regge theory. The hard gluon–gluon scattering and semi-hard processes with quark and gluon interactions are also incorporated in the model, i.e., the eikonal $u(s,b)$ consists of two terms

$$u(s,b) = u_{\rm soft}(s,b) + u_{\rm hard}(s,b). \tag{1}$$

Here b is the impact parameter of the collision. Recall that the inelastic hadronic cross section $\sigma_{\rm inel}(s)$ is connected to the real part of the eikonal $u^R(s,b)$ as

$$\sigma_{\rm inel}(s) = 2\pi \int\limits_0^\infty \left\{1 - \exp\left[-2u^R(s,b)\right]\right\} b\,db. \tag{2}$$

The inclusive spectra in the QGSM automatically have the correct triple-Regge limit for Feynman variable $x \to 1$, double-Regge limit for $x \to 0$, and satisfy all conservation laws. For the modeling of string fragmentation the Field–Feynman algorithm [6] is employed. It enables one to consider emission of hadrons from both ends of the string with equal probabilities. The break-up procedure invokes the energy–momentum conservation and the preservation of the quark numbers. Further details can be found in [4].

2. RESULTS AND CONCLUSIONS

One of the first LHC results for pp collisions was the observation of nonlinear rise of midrapidity density of charged particles with increasing $\ln s$. In contrast, at energies below 900 GeV the variation of $dN/d\eta$ at $\eta = 0$ with $\ln s$ can be approximated to linear

dependence. The charged particle pseudorapidity spectra $dN/d\eta$ calculated in QGSM for inelastic and non-single diffractive (NSD) pp collisions are shown in Fig. 1 together with the $pp(\bar{p}p)$ experimental data at energies varying from $\sqrt{s} = 200$ GeV to 7 TeV. The difference between the pp and $\bar{p}p$ collisions at such high energies is negligible, because the annihilation cross section drops almost to zero. One can see that the model reproduces the experimental results quite well. Predictions for the top LHC energy $\sqrt{s} = 14$ TeV are also displayed in Fig. 1. According to QGSM, the density of charged particles at midrapidity should rise further to

$$\left.\frac{dN_{\rm inel}}{d\eta}\right|_{\eta=0} = 6.2, \qquad \left.\frac{dN_{\rm NSD}}{d\eta}\right|_{\eta=0} = 7.1.$$

In other words, the hypothesis of Feynman scaling, which postulates the independence of particle density from $\sqrt{s}$, is not fulfilled even at top LHC energies.

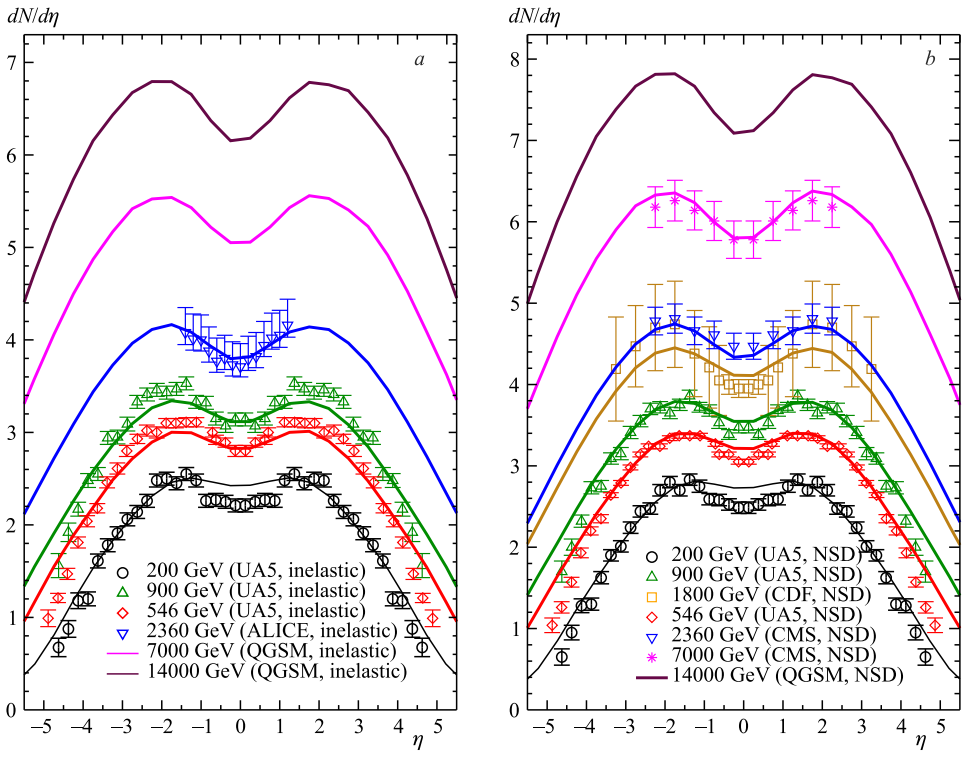

Fig. 1. The charged particle pseudorapidity spectra for inelastic (*a*) and non-single diffractive (*b*) events calculated in QGSM for pp collisions at $\sqrt{s}$ from 200 GeV to 14 TeV. Data are taken from [7–9]

Figure 2 presents the transverse momentum spectra of charged particles produced in NSD events. Again, the QGSM calculations are confronted to available experimental data, and the agreement between the model results and the data is very good. The spectra become harder with rising $\sqrt{s}$ mainly due to the contribution of hard Pomeron processes. This leads to the increase of average transverse momentum of secondaries. For instance, at $\sqrt{s} = 900$ GeV

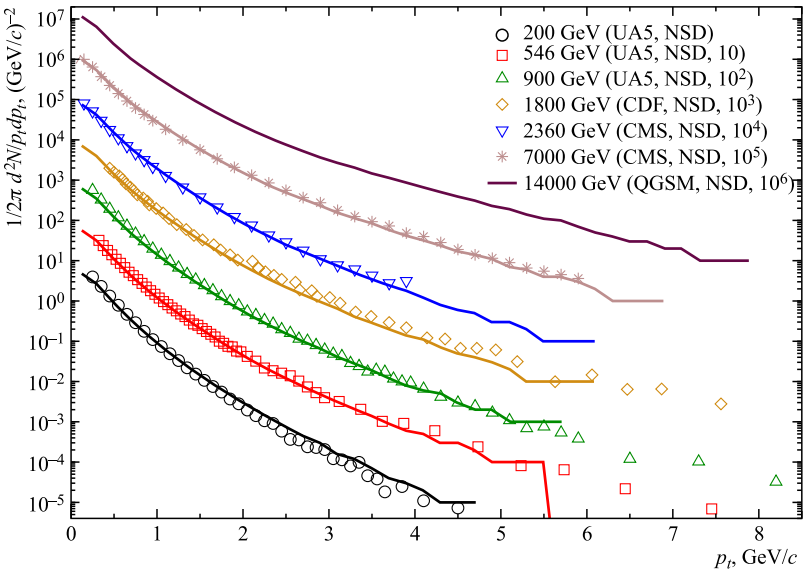

Fig. 2. Transverse momentum distributions of the invariant cross section of charged particles in NSD pp collisions obtained in QGSM at $|y| \leqslant 2.5$ for all energies in question. Data are taken from [7, 9]

the particles with the transverse momentum $p_T \leqslant 2.8$ GeV/c are produced mainly in soft processes. At $\sqrt{s} = 2360$ GeV the hard processes, or minijets, start to dominate over the soft ones already at $p_T \geqslant 2.2$ GeV/c.

Finally, multiplicity distributions of charged particles in NSD events are shown in Fig. 3 for $\sqrt{s} = 900$ GeV and 2.36 TeV. For all three pseudorapidity bins the agreement between the model calculations and the data is good. Moreover, wavy fluctuations at $N_{\rm ch} \geqslant 25$ are distinctly seen in the larger η intervals both in the data and in the QGSM. In the experiment these peculiarities can be explained perhaps by fluctuations in the raw data [8], but in the

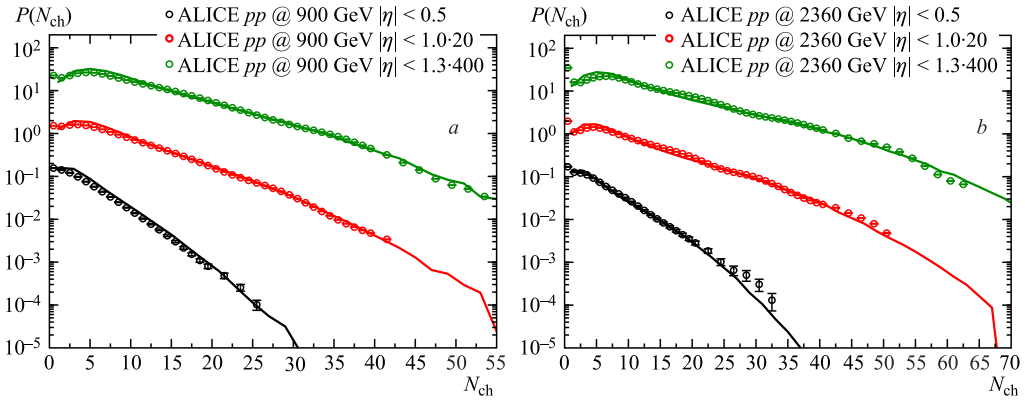

Fig. 3. Multiplicity distributions in three η intervals for NSD collisions at $\sqrt{s} = 900$ GeV (a) and at 2.36 TeV (b). Data are taken from [8]

model such behavior is linked to the many-Pomeron processes. At lower energies their contributions to particle multiplicity strongly overlap, whereas at $\sqrt{s} \geqslant 900$ GeV the maxima of the distributions for n-Pomeron processes are shifted to higher multiplicities, thus causing the wavy profile of the spectra.

In conclusion, the MC version of the quark–gluon string model with soft and hard Pomeron exchanges is considered. The model is able to describe general characteristics of particle production in ultrarelativistic pp collisions in a broad energy range. Predictions are made for the top LHC energy $\sqrt{s} = 14$ TeV. Analysis of femtoscopic correlations, which can provide valuable information about the space-time picture of particle production in the model, is done in the subsequent paper [10].

REFERENCES

1. *Gribov V.* // Sov. Phys. JETP. 1968. V. 26. P. 414;
   Gribov L. V., Levin E. M., Ryskin M. G. // Phys. Rep. 1983. V. 100. P. 1.
2. *Kaidalov A. B.* // Phys. Lett. B. 1982. V. 116. P. 459;
   Kaidalov A. B., Ter-Martirosyan K. A. // Phys. Lett. B. 1982. V. 117. P. 247.
3. *Capella A. et al.* // Phys. Rep. 1994. V. 236. P. 225.
4. *Amelin N. S., Bravina L. V.* // Sov. J. Nucl. Phys. 1990. V. 51. P. 133;
   Bleibel J. et al. arXiv:1011.2703 [hep-ph].
5. *Abramovskii V., Gribov V., Kancheli O.* // Sov. J. Nucl. Phys. 1974. V. 18. P. 308.
6. *Field R. D., Feynman R. P.* // Nucl. Phys. B. 1978. V. 136. P. 1.
7. *Alner G. J. et al. (UA5 Collab.)* // Phys. Rep. 1987. V. 154. P. 247.
8. *Aamodt K. et al. (ALICE Collab.)* // Eur. Phys. J. C. 2010. V. 68. P. 89, P. 345.
9. *Khachatryan K. et al. (CMS Collab.)* // Phys. Rev. Lett. 2010. V. 105. P. 022002.
10. *Nilsson M. S. et al.* // Part. Nucl., Lett. Heavy Ions. 2011. V. 8, No. 9.